Hindawi Publishing Corporation
Journal of Spectroscopy
Volume 2016, Article ID 5396439, 15 pages
http://dx.doi.org/10.1155/2016/5396439

Research Article

Spectroscopic Investigations and DFT Calculations on 3-(Diacetylamino)-2-ethyl-*3H*-quinazolin-4-one

Yusuf Sert,[1,2] Fatih Ucun,[3] Gamal A. El-Hiti,[4] Keith Smith,[5] and Amany S. Hegazy[5]

[1] *Department of Physics, Faculty of Art & Sciences, Bozok University, 66100 Yozgat, Turkey*
[2] *Sorgun Vocational School, Bozok University, 66100 Yozgat, Turkey*
[3] *Department of Physics, Faculty of Art & Sciences, Süleyman Demirel University, 32100 Isparta, Turkey*
[4] *Cornea Research Chair, Department of Optometry, College of Applied Medical Sciences, King Saud University, P.O. Box 10219, Riyadh 11433, Saudi Arabia*
[5] *School of Chemistry, Cardiff University, Main Building, Park Place, Cardiff CF10 3AT, UK*

Correspondence should be addressed to Gamal A. El-Hiti; gelhiti@ksu.edu.sa

Received 23 October 2015; Accepted 28 January 2016

Academic Editor: Christoph Krafft

The theoretical and experimental vibrational frequencies of 3-(diacetylamino)-2-ethyl-3*H*-quinazolin-4-one (**2**) were investigated. The experimental Laser-Raman spectrum (4000–100 $\mathrm{cm^{-1}}$) and FT-IR spectrum (4000–400 $\mathrm{cm^{-1}}$) of the newly synthesized compound were recorded in the solid phase. Both the theoretical vibrational frequencies and the optimized geometric parameters such as bond lengths and bond angles have for the first time been calculated using density functional theory (DFT/B3LYP and DFT/M06-2X) quantum chemical methods with the 6-311++G(d,p) basis set using Gaussian 03 software. The vibrational frequencies were assigned with the help of potential energy distribution (PED) analysis using VEDA 4 software. The calculated vibrational frequencies and the optimized geometric parameters were found to be in good agreement with the corresponding reported experimental data. Also, the energies of the lowest unoccupied molecular orbital (LUMO), highest occupied molecular orbital (HOMO), and other related molecular energies for 3-(diacetylamino)-2-ethyl-3*H*-quinazolin-4-one (**2**) have been investigated using the same computational methods.

1. Introduction

Quinazoline derivatives are of interest because they show a variety of biological activities including anti-inflammation [1], antibacterial [2], antispasm [3], anticancer [4, 5], antiobesity [6] and reductase inhibitory properties [7]. Quinazolin-4-one derivatives have been synthesized by various methods, for example, reactions of carbon dioxide with 2-aminobenzonitrile without use of a catalyst in water [8]; reactions of *N*-substituted 2-bromobenzamides with formamide catalysed by CuI and 4-hydroxy-l-proline [9]; three-component reactions of benzyl halides, isatoic anhydride, and primary amines under mild Kornblum conditions [10]. We have shown that the quinazoline ring system can be easily modified *via* lithiation by a lithium reagent such as alkyllithium in anhydrous tetrahydrofuran at low temperature followed by reactions with electrophiles to provide access to substituted derivatives in high yields. Such derivatives might be difficult to synthesize by other means [11–15].

As far as we are aware, there have been no previous reports of quantum chemical calculations or FT-IR and Laser-Raman spectral studies on 3-(diacetylamino)-2-ethyl-3*H*-quinazolin-4-one (**2**). Herein, we report experimental infrared and Raman spectra along with quantum chemical calculations, which correlate well with each other, to enable vibrational frequencies for compound **2** to be assigned.

2. Experimental Details

2.1. Characterization Techniques. FT-IR spectra over the range 4000–400 $\mathrm{cm^{-1}}$ were obtained on solid phase samples at room temperature using a Perkin-Elmer Spectrum Two FT-IR Spectrometer with 4 $\mathrm{cm^{-1}}$ resolution. Raman spectra within the range of 4000–100 $\mathrm{cm^{-1}}$ were obtained on solid phase samples using a Renishaw inVia Raman microscope (excitation line at 785 nm from a diode laser; 100 scans, resolution 1 cm^{-1}).

Melting point determination was performed on a Gallenkamp melting point apparatus by the open capillary method. ^{1}H (500 MHz) and ^{13}C NMR (125 MHz) spectra were recorded on a Bruker AV500 spectrometer in deuterated dimethyl sulfoxide (DMSO-d_6). Chemical shifts δ (ppm) are reported relative to tetramethylsilane (TMS) and coupling constants (J) are in Hz. DEPT spectra were used to detect the ^{13}C multiplicities. Coupling patterns, integration values, and expected chemical shifts were used to assign signals. The low and high-resolution mass spectra were recorded on Waters GCT Premier and Waters LCT Premier XE instruments, respectively. A Nonius Kappa CCD diffractometer was used to record the X-ray single-crystal diffraction data by the use of graphite-monochromated Mo-K$_\alpha$, (λ = 0.71073 Å) radiation. The structure was solved by direct methods using SHELXS-96 [16] and refined with all data on F^2 full-matrix least squares using SHELXL-97 [17]. The full crystallographic data (CCDC 971829) for the title compound can be obtained *via* http://www.ccdc.cam.ac.uk/structures.

2.2. Chemicals. Chemicals and reagents from Sigma-Aldrich were used without further purification and Fischer Scientific silica 60A (35–70 micron) was used in the purification of **2** by column chromatography.

*2.3. Synthesis of 3-(Diacetylamino)-2-ethyl-3H-quinazolin-4-one (**2**).* Acetic anhydride (Ac_2O; 2.1 mL, 22.0 mmol) in anhydrous toluene (5 mL) was added to a stirred mixture of 3-amino-2-ethyl-3*H*-quinazolin-4-one (**1**; 1.89 g, 10.0 mmol) and triethylamine (TEA; 5 mL) in dry toluene (20 mL) (Scheme 1). The mixture was refluxed for 30 min, allowed to cool, washed twice with saturated aq. $NaHCO_3$ (10 mL) and water (15 mL), and dried ($MgSO_4$), and the solvent was evaporated under vacuum. Column chromatography (silica; Et_2O-hexane, 1 : 4) was used to purify the crude product to give a white powder. Crystallization from ethyl acetate provided colorless crystals of **2** (2.58 g, 9.4 mmol; 94%); m.p. 110–111°C. ^{1}H NMR (500 MHz, DMSO-d_6, δ, ppm): 8.16 (dd, J = 8.0, 1.2 Hz, 1 H, H-5), 7.94 (app. dt, J = 1.2, 8.0 Hz, 1 H, H-7), 7.76 (br app. d, J = 8.0 Hz, 1 H, H-8), 7.61 (app. dt, J = 1.2, 8.0 Hz, 1 H, H-6), 2.67 (q, J = 7.2 Hz, 2 H, CH_2), 2.40 (s, 6 H, 2 $CH_3C{=}O$), 1.26 (t, J = 7.2 Hz, 3 H, CH_3CH_2). ^{13}C NMR (125 MHz, DMSO-d_6, δ, ppm): 170.8 (s, 2 C=O), 159.4 (s, C-4), 158.0 (s, C-2), 146.9 (s, C-8a), 136.2 (d, C-7), 128.0 (d, C-5), 127.8 (d, C-6), 127.2 (d, C-8), 120.7 (s, C-4a), 25.7 (t, CH_2), 24.9 (q, 2 $CH_3C{=}O$), 10.4 (q, CH_3CH_2). CI-MS: (m/z, %): = 274 ($[MH]^+$, 100). HRMS (CI): Calculated for $C_{14}H_{16}N_3O_3$ $[MH]^+$ 274.1192; found: 274.1201.

3. Computational Details

The use of density functional theory (DFT) calculations has increased rapidly for various applications, particularly since accurate nonlocal corrections were introduced. The methods employed in the current work have been used in many previous theoretical studies [18–32].

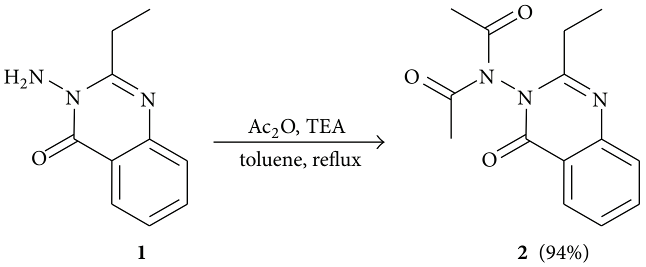

Scheme 1: Synthesis of 3-(diacetylamino)-2-ethyl-3*H*-quinazolin-4-one (**2**).

Initial atomic coordinates can generally be taken from experimental XRD results or a database. In this work, experimental XRD data and the Gauss View software database have each been used to determine initial atomic coordinates and to optimize the input structure. The most stable structure after optimization was obtained from the initial atomic coordinates taken from the Gauss View database [33]. This most stable structure, following optimization, was used for further theoretical analysis. The calculated gas phase ground state molecular structure of the title compound was optimized by the use of DFT/B3LYP and DFT/M06-2X methods with the 6-311++G(d,p) basis set, and the calculated optimized structure was used in the vibrational frequency calculations. The calculated harmonic vibrational frequencies were scaled by 0.9614 (B3LYP) and 0.9489 (M06-2X) for use with the 6-311++G(d,p) basis set, respectively [33, 34]. Identical scale factors were used for the entire spectra. The Gauss View molecular visualization program [33] and the Gaussian 03 program [35] were used to calculate vibrational wavenumbers, optimized geometric parameters, and other molecular properties. The calculated vibrational frequencies were assigned *via* potential energy distribution (PED) analysis of all the fundamental vibration modes by the use of the VEDA 4 program [36, 37] that has been used previously [20, 23, 24, 32, 38, 39]. All the vibrational assignments were based on the B3LYP/6-311++G(d,p) level calculations. Consequently, some assignments could correspond to the value of the next or previous vibrational frequency at the M06-2X/6-311++G(d,p) level.

4. Results and Discussion

4.1. Synthesis. 3-(Diacetylamino)-2-ethyl-3*H*-quinazolin-4-one (**2**) was synthesized, in 94% yield after crystallization, by double acetylation of 3-amino-2-ethyl-3*H*-quinazolin-4-one (**1**) with acetic anhydride (two mole equivalents) in boiling toluene for 3 h in the presence of triethylamine (Scheme 1). Various spectroscopic techniques were used to confirm the structure of **2**.

4.2. Geometric Structure. The single-crystal X-ray crystallographic analysis of **2** ($C_{14}H_{15}N_3O_3$) showed that the crystal belonged to the monoclinic system and the $P2_1/c$ space group and possessed the following cell dimensions: a = 7.4975 Å,

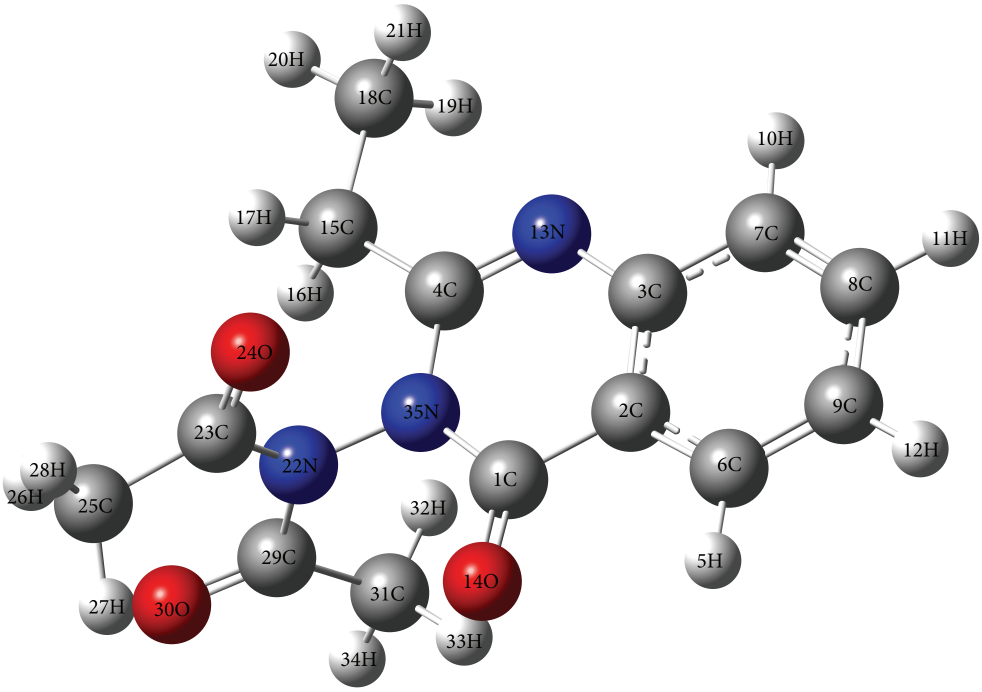

Figure 1: The optimized molecular structure of compound **2**.

$b = 12.0246$ Å, and $c = 15.1939$ Å and $\alpha = 90^\circ$, $\beta = 97.399^\circ$, $\gamma = 90^\circ$, and $V = 1358.39$ Å^3. The measured density of compound **2** was 1.336 mg/mm^3. Table 1 shows the bond lengths and bond angles for the optimized theoretical and experimental structures along with the atom numbering scheme (Figure 1).

As can be seen from Table 1, the optimized parameters calculated at both DFT levels differ only slightly from the experimental values, and small variations are to be expected since the calculations correspond to the gas phase rather than the solid state. For example, in the quinazoline moiety, the C4–N13 and C4–N35 bond lengths are calculated as 1.286 and 1.401 Å, respectively, by the B3LYP method, and 1.280 and 1.397 Å, respectively, by the M06-2X method, while the experimental values are 1.286 and 1.400 Å, respectively. Similarly, the N13–C4–N35 and C4–N35–C1 bond angles were calculated as 121.9 and 123.6°, respectively, by the B3LYP method and 122.3 and 123.9°, respectively, by the M06-2X method, while the experimental bond angles were 121.7 and 124.5°, respectively.

In order to quantify the level of agreement between the experimental and computational results, correlation coefficients (R^2) for linear regression analysis of the experimental and theoretical bond angles and lengths were calculated (last row in each section of Table 1). The values are 0.9820/0.9799 for bond lengths and 0.9596/0.9599 for bond angles for B3LYP/M06-2X. These values show that bond lengths calculated using the B3LYP method are slightly closer to the experimental data, but bond angles calculated using the M06-2X method are marginally closer to the data obtained experimentally.

The largest variations between the experimental and calculated (B3LYP/6-311++G(d,p)) bond lengths are 0.016 Å for the C1–N35 bond; 0.011 Å for the C3–N13 bond; 0.018 Å for the C8-C9 bond; 0.013 Å for the C15–C18 and C23–C25 bonds; and 0.015 Å for the C29-C31 bond. For bond angles the largest differences are 0.8° for N13–C4–C15; 0.9° for C23–N22–C29, C29–N22–N35, and C1–N35–C4; and 0.6° for C4–N35–N22.

The values found or calculated for **2** are consistent with values found experimentally or computationally for corresponding bonds and angles in related compounds such as 2-ethyl-3*H*-quinazoline-4-thione (experimental values available [40]), 3-amino-2-phenyl-3*H*-quinazolin-4-one (values calculated using the B3LYP/6-31G*, B3LYP/6-311++G(d,p), and M06-2X methods available [41]), 3-(4-methoxybenzylideneamino)-2-phenyl-3*H*-quinazolin-4-one (values calculated using the B3LYP/6-31G* basis set available [42]), methyl 3,5-dibromo-2-diacetylaminobenzoate (experimental data available [43]), and *N*-(1-diacetylamino-1*H*-tetrazol-5-yl)acetamide (experimental data available [44]).

4.3. Vibrational Analysis. As seen from Figure 1, the molecule has 35 atoms, so there are 105 motions, 3 of which are translational, 3 of which are rotational, and 99 of which are vibration modes. The molecule has C_1 symmetry. The experimental FT-IR and Laser-Raman spectra of compound **2** are compared with the selected theoretical spectra in Figures 2 and 3, respectively (identified bands are those discussed in the text and bold numbers in Table 2). The observed vibrational frequencies, scaled harmonic vibrational frequencies calculated at both B3LYP and M06-2X levels, and

Table 1: Experimental and calculated geometric parameters of compound **2** (figures in bold relate to parameters discussed in the text).

Geometric parameters	Experimental values	Calculated values	
		B3LYP/6-311++G(d,p)	M06-2X/6-311++G(d,p)
Bond lengths (Å)			
C1–C2	1.458	1.461	1.462
C1–O14	1.216	1.216	1.209
C1–N35	1.406	1.422	1.411
C2–C3	1.399	1.409	1.402
C2–C6	1.403	1.403	1.399
C3–C7	1.402	1.407	1.403
C3–N13	1.398	1.387	1.389
C4–N13	**1.286**	**1.286**	**1.280**
C4–C15	1.499	1.509	1.505
C4–N35	**1.400**	**1.401**	**1.397**
H5–C6	0.93	1.083	1.084
C6–C9	1.375	1.383	1.380
C7–C8	1.372	1.384	1.381
C7–H10	0.93	1.083	1.083
C8–C9	1.387	1.405	1.403
C8–H11	0.93	1.084	1.084
C9–H12	0.93	1.084	1.083
C15–H16	0.97	1.096	1.095
C15–H17	0.97	1.095	1.095
C15–C18	1.515	1.528	1.522
C18–H19	0.96	1.091	1.090
C18–H20	0.96	1.093	1.091
C18–H21	0.96	1.090	1.089
N22–C23	1.422	1.442	1.433
N22–C29	1.417	1.421	1.416
N22–N35	1.401	1.395	1.383
C23–O24	1.201	1.207	1.201
C23–C25	1.490	1.503	1.499
C25–H26	0.96	1.091	1.089
C25–H27	0.96	1.090	1.089
C25–H28	0.96	1.089	1.088
C29–O30	1.201	1.208	1.201
C29–C31	1.496	1.511	1.508
C31–H32	0.96	1.092	1.092
C31–H33	0.96	1.092	1.092
C31–H34	0.96	1.088	1.087
R^2		**0.982**	**0.9799**
Bond angles (°)			
C2–C1–O14	126.6	126.5	126.6
C2–C1–N35	112.9	113.1	112.8
O14–C1–N35	120.5	120.4	120.5
C1–C2–C3	119.3	119.3	119.3
C1–C2–C6	120.2	120.1	119.8
C3–C2–C6	120.4	120.6	120.9
C2–C3–C7	118.9	118.8	118.7
C2–C3–N13	122.9	122.6	122.8
C7–C3–N13	118.1	118.6	118.4

Table 1: Continued.

Geometric parameters	Experimental values	Calculated values	
		B3LYP/6-311++G(d,p)	M06-2X/6-311++G(d,p)
N13–C4–C15	121.5	120.7	121.1
N13–C4–N35	**121.7**	**121.9**	**122.3**
C15–C4–N35	116.8	117.3	116.5
C2–C6–H5	120.3	118.6	118.5
C2–C6–C9	119.5	119.8	119.6
H5–C6–C9	119.9	121.6	121.9
C3–C7–C8	119.8	120.1	120.1
C3–C7–H10	120.1	118.3	118.1
C8–C7–H10	120.1	121.6	121.8
C7–C8–C9	121.2	120.7	120.9
C7–C8–H11	119.4	119.6	119.6
C9–C8–H11	119.9	119.6	119.5
C6–C9–C8	120.1	119.9	119.8
C6–C9–H12	119.9	120.2	120.2
C8–C9–H12	119.9	119.9	119.9
C3–N13–C4	121.7	119.4	118.7
C4–C15–H16	108.9	109.0	108.8
C4–C15–H17	108.9	107.8	107.5
C4–C15–C18	113.3	113.7	112.7
H16–C15–H17	107.7	105.7	106.1
H16–C15–C18	108.9	110.1	110.8
H17–C15–C18	108.9	110.1	110.6
C15–C18–H19	109.5	111.4	110.9
C15–C18–H20	109.5	109.5	109.7
C15–C18–H21	109.5	111.1	110.7
H19–C18–H20	109.5	108.6	108.9
H19–C18–H21	109.5	107.5	107.6
H20–C18–H21	109.5	108.6	108.9
C23–N22–C29	127.8	126.9	127.1
C23–N22–N35	114.0	114.1	114.0
C29–N22–N35	117.2	118.1	117.8
N22–C23–O24	118.4	117.9	117.8
N22–C23–C25	118.4	118.8	118.4
O24–C23–C25	123.3	123.4	123.8
C23–C25–H26	109.5	111.1	110.7
C23–C25–H27	109.5	111.2	110.7
C23–C25–H28	109.5	106.9	106.7
H26–C25–H27	109.5	106.6	106.9
H26–C25–H28	109.5	110.5	110.8
H27–C25–H28	109.5	110.7	110.9
N22–C29–O30	120.5	120.9	121.1
N22–C29–C31	116.7	116.3	115.5
O30–C29–C31	122.8	122.9	123.4
C29–C31–H32	109.5	112.2	111.5
C29–C31–H33	109.5	110.2	109.8
C29–C31–H34	109.5	107.3	107.3
H32–C31–H33	109.5	108.1	108.3
H32–C31–H34	109.5	109.6	110.0
H33–C31–H34	109.5	109.6	109.9
C1–N35–C4	**124.5**	**123.6**	**123.9**

Table 1: Continued.

Geometric parameters	Experimental values	Calculated values	
		B3LYP/6-311++G(d,p)	M06-2X/6-311++G(d,p)
C1–N35–N22	116.1	115.9	115.9
C4–N35–N22	119.2	119.8	119.4
R^2		**0.9596**	**0.9599**

Table 2: Observed and calculated vibrational frequencies of title compound with 6-311++G(d,p).

Vibration number	Assignment (PED%)[a]	Observed frequencies		Calculated frequencies in cm^{-1}	
		FT-IR	Laser-Raman	B3LYP	M06-2X
ν_1	υCH (93) in ring 1	3083	3079	3078	3057
ν_2	υCH (98) in ring 1	3083	3079	3074	3052
ν_3	υCH (89) in ring 1	3083	3079	3063	3042
ν_4	υCH (94) in ring 1	3045	3079	3048	3028
ν_5	υCH (91) in asymm. str. CH$_3$	3045	3079	3033	3025
ν_6	υCH (99) in asymm. str. CH$_3$	3045	3079	3032	3024
ν_7	υCH (100) in asymm. str. CH$_3$	**3003**	**2993**	**3009**	**3006**
ν_8	υCH (65) in asymm. str. CH$_3$	**3003**	**2993**	**3003**	**2988**
ν_9	υCH (99) in asymm. str. CH$_3$	**3003**	**2993**	**2996**	**2987**
ν_{10}	υCH (99) in asymm. str. CH$_3$	**3003**	**2993**	**2989**	**2977**
ν_{11}	υCH (85) in symm. str. CH$_3$	2949	2938	2943	2929
ν_{12}	υCH (92) in asymm. str. CH$_2$	2934	2938	2939	2922
ν_{13}	υCH (99) in symm. str. CH$_3$	2934	2938	2934	2916
ν_{14}	υCH (98) in symm. str. CH$_3$	2934	2914	2928	2904
ν_{15}	υCH (94) in symm. str. CH$_2$	**2915**	**2914**	**2911**	**2888**
ν_{16}	υOC (72) in C23–O24 and C29–O30	1735	1743	1720	1764
ν_{17}	υOC (92) in C23–O24 and C29–O30	**1725**	**1725**	**1718**	**1721**
ν_{18}	υOC (72) in O14–C1	**1693**	**1694**	**1683**	**1721**
ν_{19}	υNC (53) in N13–C4 + υCC (18) in ring 1	**1605**	**1609**	**1593**	**1623**
ν_{20}	υCC (47) in ring 1 + υNC (14) in N13–C4 + δCCC (10) in ring 1	**1570**	**1578**	**1580**	**1601**
ν_{21}	υCC (53) in ring 1 + δCCC (30) in ring 1	1514		1539	1559
ν_{22}	δHCH (67) in the CH$_3$ asym. def. and CH$_3$ twisting mode	1442	1455	1446	1445
ν_{23}	δHCC (39) in ring 1 + δCCC (22) in ring 1	1442	1431	1444	1436
ν_{24}	δHCH (70) in CH$_3$ asymm. def. + τHCCN (14) in H17–C15–C4–N13	1426	1431	1436	1425
ν_{25}	υCC (37) in ring 1 + δHCC (34) in ring 1	1426	1431	1435	1417
ν_{26}	δHCH (58) in CH$_3$ asymm. def. + τHCCN (13) in H33–C31–C29–N22	1426	1431	1429	1415
ν_{27}	δHCH (74) in CH$_3$ asymm. def. + τHCCN (13) in H33–C31–C29–N22	1409	1406	1414	1405
ν_{28}	δHCH (72) in CH$_3$ asymm. def.	1409	1406	1413	1402
ν_{29}	δHCH (84) in CH$_2$ sciss.	1409	1406	1406	1389
ν_{30}	δHCH (68) in CH$_3$ asymm. def.	1409	1382	1398	1384
ν_{31}	δHCH (79) in CH$_3$ symm. Def.	1364	1363	1366	1353
ν_{32}	δHCH (81) in CH$_3$ symm. Def.	1364	1363	1349	1344
ν_{33}	δHCH (60) in CH$_3$ symm. Def.	1328	1333	1344	1339
ν_{34}	τHCCN (33) in H17–C15–C4–N13 and CH$_2$ wagging mode in the ethyl group	1328	1333	1337	1331

Table 2: Continued.

Vibration number	Assignment (PED%)[a]	Observed frequencies		Calculated frequencies in cm^{-1}	
		FT-IR	Laser-Raman	B3LYP	M06-2X
ν_{35}	υCC (72) in ring 1	1295		1304	1304
ν_{36}	υNN (12) in N22–N35	1295	1272	1272	1292
ν_{37}	δHCC (28) in ring 1 + υNC (11) in N13–C3 + υCC (10) in ring 1 + υNNv (10) in N22–N35	1263	1272	1268	1260
ν_{38}	δHCC (63) in H17–C15–C18 and H21–C18–C15 and twisting mode CH$_2$ in the ethyl group + τHCCN (14) in H17–C15–C4–N13	1240	1247	1246	1246
ν_{39}	υNC (13) in N13–C3 and N22–C29	**1240**	**1230**	**1235**	**1227**
ν_{40}	υCC (11) in ring 1 + δHCC (10) in ring 1 + δCCC (10) in ring 1	1214	1230	1208	1218
ν_{41}	υNC (28) in C1–N35 and N22–C23	**1188**	**1192**	**1190**	**1198**
ν_{42}	υNC (24) in C1–N35 and N22–C23 + δHCC (11) in ring 1	1188	1192	1180	1195
ν_{43}	δHCC (10) in ring 1 and H28–C25–C23 + υNN (10) in N22–N35	1149	1149	1157	1168
ν_{44}	δHCC (56) in ring 1	1110	1100	1127	1109
ν_{45}	δHCC (38) in ring 1 + δCCC (10) in ring 1	1100	1100	1089	1082
ν_{46}	υCC (23) in C18–C15	1058		1069	1076
ν_{47}	τHCCN (43) in H17–C15–C4–N13 + δHCH (10) in H17–C15–H16 and H21–C18–H19	1058		1062	1045
ν_{48}	τHCCC (10) in CH$_3$ rocking + τHCCN (10) in H33–C31–C29–N22	1038	1026	1035	1038
ν_{49}	τHCCC (38) in CH$_3$ rocking + γONCC (12) in O24–C23–N22–N35 + δHCH (12) in H28–C25–H27	1025	1026	1019	1019
ν_{50}	τHCCN (41) in H32–C31–C29–N22 + δHCH (13) in H33–C31–C32	1025	1026	1017	1012
ν_{51}	τHCCN (20) in H33–C31–C29–N22	1025	1026	1012	1009
ν_{52}	τHCCN (13) in H17–C15–C4–N13	1025	1026	1009	1005
ν_{53}	υCC (33) in ring 1	979	990	998	999
ν_{54}	τHCCC (83) in ring 1 out of plane H	970		969	972
ν_{55}	τHCCC (74) in ring 1 out of plane H + τCCCC (11) in ring 1 out of plane C	944	947	951	956
ν_{56}	υCC (25) in C18–C15 and C25–C23 + τHCCC (10) in the H20–C18–C15–C4/CH$_3$ rocking mode	944		948	955
ν_{57}	υCC (32) in C18–C15 and C25–C23	944		910	918
ν_{58}	υCC (40) in C29–C31	878	879	898	910
ν_{59}	τHCCC (77) in ring 1 out of ring H + γNCCC (10) in N13–C3–C7–C2	878	879	862	864
ν_{60}	δCCC (31) in ring 1 + υNC (10) in N13–C3	878	879	856	849
ν_{61}	τHCCN (42) in H17–C15–C4–N13 and rocking mode CH$_3$ in the ethyl group + γCNNC (12) in C1–N35–C4–N13	803	794	782	784
ν_{62}	υNC (11) in C4–N35 + υCC (10) in C23–C25	774	769	777	775
ν_{63}	γONCC (24) in O14–N35–C1–C2 + τHCCC (16) + τCCCC (12)	774		774	767
ν_{64}	τHCCC (51) out of ring H + τCNCC (10) in C4–N35–C1–C2	774		757	752
ν_{65}	τCCCC (18) out of ring 1 C + τHCCC (15) out of ring 1 H	680		682	677
ν_{66}	τCCCC (26) out of ring 1 C	660	665	659	657
ν_{67}	δCCC (48) in ring 1 and C4–C15–C18	647	647	649	648

Table 2: Continued.

Vibration number	Assignment (PED%)[a]	Observed frequencies		Calculated frequencies in cm^{-1}	
		FT-IR	Laser-Raman	B3LYP	M06-2X
ν_{68}	υCC (16) in C2–C3 + δOCC (15) in O24–C23–C25	618		624	626
ν_{69}	τCNCN (20) in C3–N13–C4–N35 + τCCCC (13) in ring 1 + τCCCN (13) in C3–C2–C1–N35 + γCNNC (12) in C1–N35–N22–C23	601	598	608	605
ν_{70}	δOCC (27) in O24–C23–C25 + υCC (11) in C15–C4	601	598	591	592
ν_{71}	γONCC (39) in O24–N22–C29–C25	572	580	584	582
ν_{72}	γONCC (15) in O24–N22–C29–C25 + δOCC (15) in O24–C23–C25	562	542	557	556
ν_{73}	γONCC (50) in O24–N22–C29–C25	543	542	551	548
ν_{74}	δCCC (14) in ring 1	520		527	526
ν_{75}	τCCCC (18) out of ring 1 + γNCCC (12) in N13–C3–C2–C6 + γCNNC (10) in C4–N3–N22–C23	520		507	503
ν_{76}	δCCC (27) in C4–C15–C18 and in ring 1	461	463	452	449
ν_{77}	τCCCC (24) out of ring 1 + γNCCC (10) in N13–C3–C2–C6	461	420	446	444
ν_{78}	τCCCC (27) out of ring 1	419		407	409
ν_{79}	δNNC (15) in N22–N35–C4 + δOCC (13) in O14–C1–C2 + υNC (11) in N22–C23			394	400
ν_{80}	δOCC (14) in O14–C1–C2 + δCCN (18) in C25–C23–N22			391	393
ν_{81}	δCCN (57) in C25–C23–N22		365	355	363
ν_{82}	δCNN (25) in C29–N22–N35 + δCCC (12) in C18–C15–C4		365	346	353
ν_{83}	δCCN (18) in C25–C23–N22 + δCCC (11) in C18–C15–C4		328	314	325
ν_{84}	τCCCC (30) out of ring 1 + γCNNC (12) in C3–C4–N35–C1		297	291	289
ν_{85}	δNCC (36) in N22–C23–C25		297	287	285
ν_{86}	τHCCN (56)		218	229	251
ν_{87}	δCNC (25) in C23–N22–C29 + δCCN (13) in C15–C4–N13 + τHCCC (10)		218	202	226
ν_{88}	τHCCC (45)		218	194	211
ν_{89}	τHCCN (83) in H33–C31–C29–N22		162	182	203
ν_{90}	τCNCC (37) in C4–N13–C3–C2 + γNCCC (15) in N13–C4–C15–C18		162	156	156
ν_{91}	δCCN (21) in C15–C4–N13 + δCCC (18) in C18–C15–C4 + δCNC (10) in C1–N35–C4		132	153	153
ν_{92}	τCNCN (35) in C3–N13–C4–N35 + γNCCN (12) in N13–C4–C15–N35		132	122	120
ν_{93}	τCNCN (25) in C3–N13–C4–N35 + γCNNC (16) + γNCCC (10) + τCCCC (10)			105	97
ν_{94}	γCNCN (52) + γNCCN (12) + τCNCN (10)			95	88
ν_{95}	τCCNN (32) + τCNCN (28) + γCNCN (10)			71	71
ν_{96}	τCCNN (71) + δNNC (14)			63	62
ν_{97}	τCCNN (61) + γNCCN (15)			60	57
ν_{98}	τCCNN (37) + γNCCN (13) + τCNCN (13)			43	44
ν_{99}	τCNCN (45) + γNCCN (29)			39	37

Table 2: Continued.

Vibration number	Assignment (PED%)[a]	Observed frequencies		Calculated frequencies in cm^{-1}	
		FT-IR	Laser-Raman	B3LYP	M06-2X
R^2				***0.9998***	***0.9997***

υ, stretching; δ, in-plane bending; γ, out-of-plane bending; τ, torsion.
[a]Potential energy distribution (PED); values less than 10% are not shown.

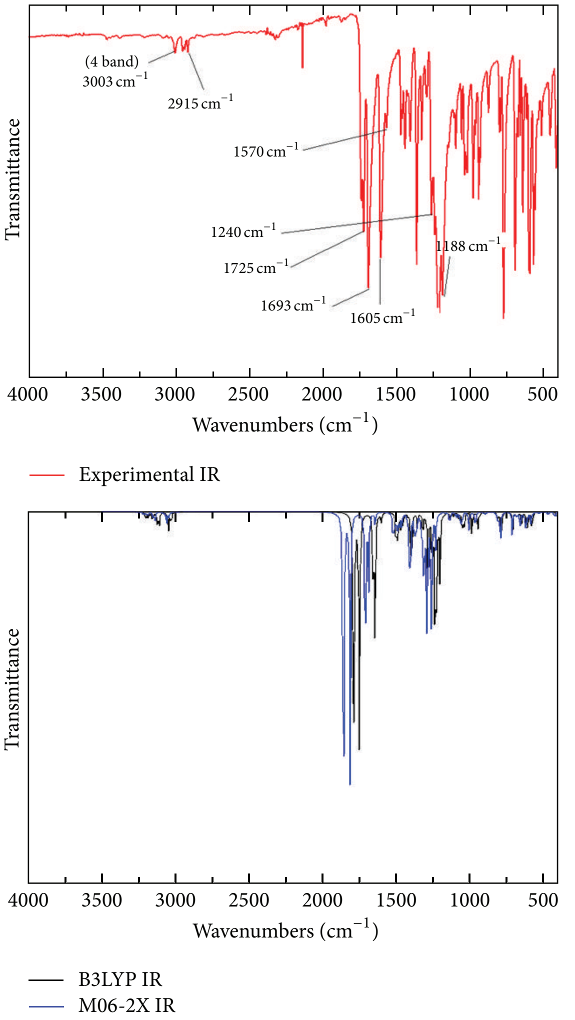

Figure 2: Comparison of observed and calculated infrared spectra of compound **2**.

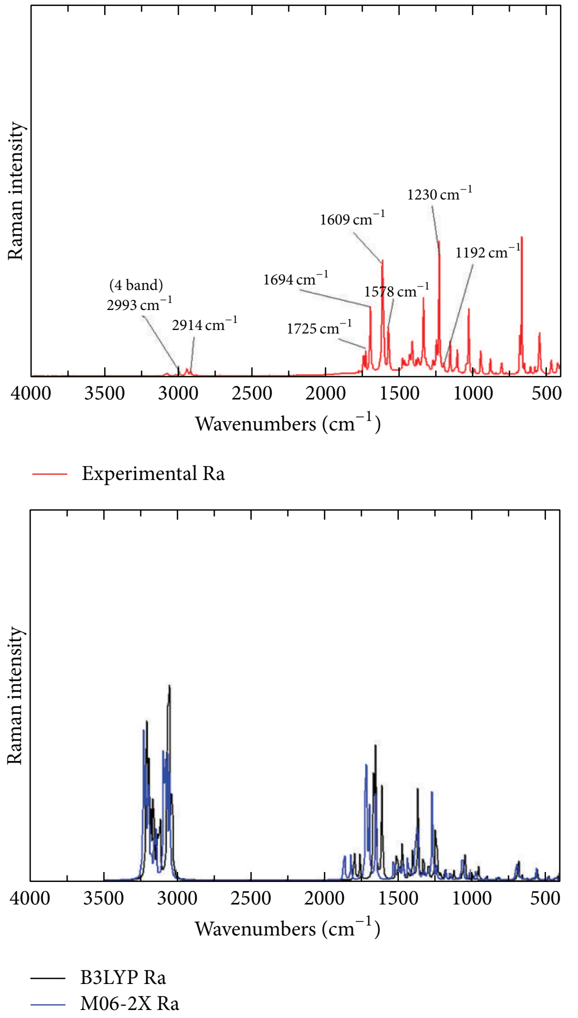

Figure 3: Comparison of observed and calculated Raman spectra of compound **2**.

detailed potential energy distribution (PED) assignments are summarized in Table 2. The harmonic frequencies calculated for the title molecule relate to the gaseous phase, but the experimental ones are obtained for the solid phase. As a result, disagreement between the calculated frequencies and some of the experimental (observed) frequencies is to be expected. A PED analysis was carried out in order to introduce detailed vibrational assignments for compound **2**. Within each fundamental wave number, the calculated modes are numbered downwards from the largest to the smallest frequency.

The harmony between the experimental and calculated wavenumbers is shown in Figure 4, which indicates that the experimental frequencies correlate well with the calculated ones, particularly for B3LYP. The relations between the experimental and calculated wavenumbers are linear and given by the following:

$$\begin{aligned} \upsilon_{\mathrm{Cal}} &= 0.9986\upsilon_{\exp} - 0.0726 \quad \text{for B3LYP method,} \\ \upsilon_{\mathrm{Cal}} &= 0.9927\upsilon_{\exp} + 5.7907 \quad \text{for M06-2X method.} \end{aligned} \tag{1}$$

The correlation coefficients (R^2 values) between the experimental and calculated wavenumbers were calculated as $R^2 = 0.9998$ for B3LYP and $R^2 = 0.9997$ for M06-2X. This indicates that the calculation methods gave reasonable agreement with the experimental values, particularly

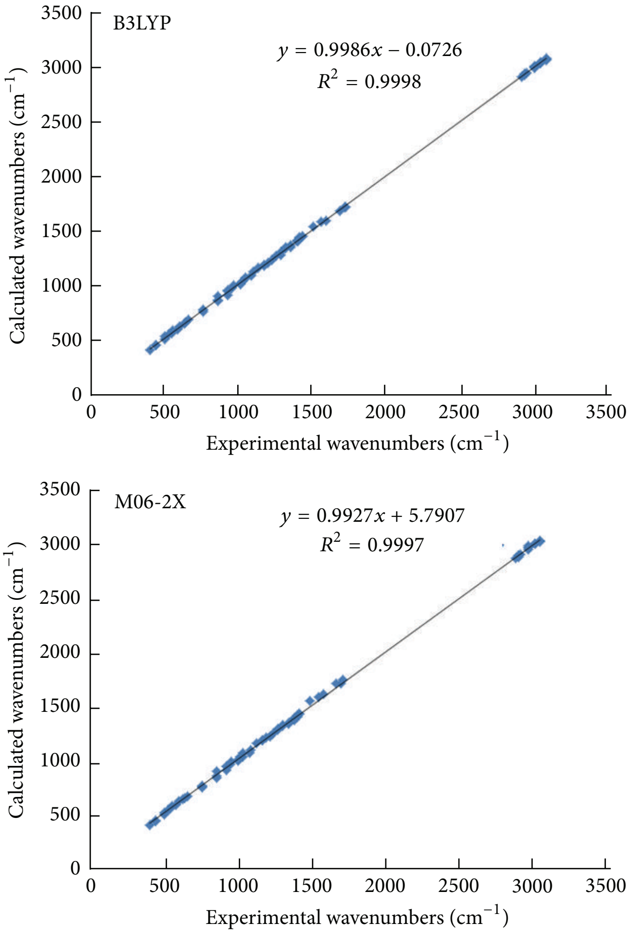

Figure 4: Correlation graphics of experimental and theoretical (scaled) wavenumbers of **2**.

in the case of the B3LYP method. However, this masks significant differences between experimental and calculated values for a few of the vibrational frequencies, which are worthy of individual mention.

4.3.1. Quinazolinone Carbonyl Group Vibrations. The carbonyl group has a strong C=O stretching vibration around 1850–1550 cm^{-1} [45]. Differences of 20–30 cm^{-1} are used to help recognize particular functional groups such as ester, ketone, or amide groups. For compound **2**, the quinazolinone νC=O mode is observed as a strong band at 1693 cm^{-1} in the IR spectrum and at 1694 cm^{-1} in the Laser-Raman spectrum. The calculated values are 1683 cm^{-1} (B3LYP) and 1721 cm^{-1} (M06-2X). This demonstrates that although the correlation coefficients R^2 are high, individual calculated frequencies can differ significantly from each other and from the experimental values, and in the case of the M06-2X method the calculated carbonyl stretching frequency differs from the experimental value by a sufficiently large margin that it could not be relied on to identify the functional group. In other cases, however, the level of agreement may be greater. For example, γONCC (O14–N35–C1–C2) is seen at 774 cm^{-1} in the IR spectrum and calculated at 774 cm^{-1} by B3LYP and 767 cm^{-1} by M06-2X. Bending modes δOCC (O14–C1–C2) were not seen in either the IR spectrum or the Raman spectrum, but two such modes were calculated to be at 394 (B3LYP)/400 (M06-2X) and 391 (B3LYP)/393 (M06-2X) cm^{-1}. For similar quinazoline derivatives [46, 47] the νC=O mode was reported at 1652 (3-{[(2-hydroxyphenyl) methylene]amino}-2-phenylquinazolin-4(3*H*)-one) and 1673 cm^{-1} (3-{[(4-fluorophenyl) methylene]amino}-2-phenylquinazolin-4(3*H*)-one) in the IR spectrum and at 1656 and 1661 cm^{-1}, respectively, in the Raman spectrum. For 3-(4-methoxybenzylideneamino)-2-phenyl-3*H*-quinazolin-4-one this mode was seen as a strong band at 1683 cm^{-1} in the IR spectrum and at 1682 cm^{-1} in the Raman spectrum and calculated to be 1690 cm^{-1} using the B3LYP/6-31G* basis set [42].

4.3.2. C15H16, 17 and C18H19, 20, 21 Group Vibrations. The CH_2 group has 6 vibrational modes (one asymmetrical and one symmetrical stretching, one scissoring, one wagging, one twisting and rocking). The asymmetric stretch $\nu_{as}CH_2$, the symmetric stretch ν_sCH_2, the scissoring vibrations δCH_2, and the wagging vibration ωCH_2 appear at 3000 ± 20, 2900 ± 25, 1440 ± 10, and 1340 ± 25 cm^{-1}, respectively [48, 49]. For compound **2**, agreement between the experimental values and those calculated by B3LYP was generally good but there was less good agreement with those calculated by M06-2X (see Table 2). For example, the CH_2 asymmetrical stretching mode was seen at 2934 cm^{-1} in the IR spectrum and 2938 cm^{-1} in the Raman spectrum. This asymmetrical stretching mode was calculated to be at 2939 (B3LYP)/2922 (M06-2X) cm^{-1}. The CH_2 symmetrical stretching mode was observed at 2915 cm^{-1} in the IR spectrum and 2914 cm^{-1} in the Raman spectrum. The symmetrical stretching mode was calculated to be at 2911 cm^{-1} by B3LYP, but 2888 cm^{-1} by M06-2X. Similarly, the CH_2 scissoring and wagging modes were seen at 1409 and 1328 cm^{-1} in the IR spectrum, and 1406 and 1333 cm^{-1} in the Laser-Raman spectrum, respectively. These modes were calculated to be at 1406 (B3LYP)/1389 (M06-2X) and 1337 (B3LYP)/1331 (M06-2X) cm^{-1}, respectively. CH_2 twisting and rocking modes appeared at 1260 ± 10 and 800 ± 25 cm^{-1}, respectively [49]. For compound **2**, the CH_2 twisting and rocking modes were seen at 1240 and 803 cm^{-1} in the IR spectrum, 1247 and 794 cm^{-1} in the Laser-Raman spectrum, respectively, and calculated to be at 1246 (B3LYP)/1246 (M06-2X) and 782 (B3LYP)/784 (M06-2X) cm^{-1}, respectively.

The CH_3 group has nine vibrational modes (two asymmetrical and one symmetrical stretching modes, two antisymmetrical deformations, one symmetrical deformation, two rocking modes, and 1 twisting mode). The CH_3 asymmetric stretching vibrations are expected in the 2950–3050 cm^{-1} region and CH_3 symmetric vibrations in the 2900–2950 cm^{-1} region [48, 49]. For compound **2** the asymmetric stretching modes were calculated to be at 3003 (B3LYP)/2988 (M06-2X) and 2989 (B3LYP)/2977 (M06-2X) cm^{-1}, and the symmetric mode at 2928 (B3LYP)/2904 (M06-2X) cm^{-1}. Asymmetric stretching modes were observed at 3003 cm^{-1} in the IR spectrum and at 2993 cm^{-1} in the Laser-Raman spectrum (the two bands appearing within a single envelope in each case), while symmetric stretching modes were observed at 2934 cm^{-1} in the IR and 2914 cm^{-1} in the Laser-Raman spectrum. Again, therefore, the B3LYP method is a better predictor of the experimental values than the M06-2X method. The same trend is observed for some of the other vibrational modes. For example, the symmetrical bending deformation, $\delta_s CH_3$, is expected at 1380 ± 25 cm^{-1} [48]. The calculated value was 1366 (B3LYP)/1353 (M06-2X) cm^{-1}, while the observed value was 1364 cm^{-1} in the IR spectrum and 1363 cm^{-1} in the Laser-Raman spectrum. Similarly, aromatic molecules display a methyl rocking in the neighborhood of 1045 cm^{-1}, and a second rocking in the region of 970 ± 70 cm^{-1}, which is more difficult to find among the C–H out-of-plane deformations [48]. For compound **2**, these ρCH_3 modes were observed at 1038 and 944 cm^{-1} in the IR spectrum; the first of these bands was observed at 1026 cm^{-1} in the Laser-Raman spectrum, but the second rocking mode was not observed. These bands were calculated at 1035 (B3LYP)/1038 (M06-2X) and 948 (B3LYP)/955 (M06-2X) cm^{-1}, respectively.

Although the M06-2X calculated frequencies of some vibrational modes were a little closer to the observed values than the ones calculated by B3LYP, in the overwhelming majority of cases B3LYP provided calculated values that were closer to the observed values (see Table 2). This perspective is more easily seen in the graphical experimental and calculated spectra shown in Figure 2 (IR) and Figure 3 (Raman). Figure 3 also reveals that the calculated intensities of some of the bands in the Raman spectra were substantially different from the experimentally observed intensities.

4.3.3. Diacetylamino Group Vibrations. For compound **2**, νC=O (C23–O24 and C29–O30) stretching modes were observed at 1735 (IR)/1743 (Raman) and 1725 (IR)/1725 (Raman) cm^{-1}, and calculated at 1720 (B3LYP)/1764 (M06-2X) and 1718 (B3LYP)/1721 (M06-2X) cm^{-1}. For 3-nitroacetanilide this mode was observed at 1676 cm^{-1} in the IR spectrum and calculated at 1774 cm^{-1} by using the HF/6-31G* method [50]. For compound **2**, two C–N stretching modes (N22–C23 and N22–C29) were observed at 1240 (IR)/1230 (Raman) and 1188 (IR)/1192 (Raman) cm^{-1}, respectively, but the latter band contained two C–N stretching frequencies within the envelope; all three frequencies were calculated, at 1235 (B3LYP)/1227 (M06-2X), 1190 (B3LYP)/1198 (M06-2X), and 1180 (B3LYP)/1195 (M06-2X) cm^{-1}.

In the acetyl group, the two CH_3 groups have 18 vibrational modes (4 asymmetrical and 2 symmetrical stretching modes, 4 antisymmetrical and 2 symmetrical deformations, 4 rocking modes, and 2 twisting modes). The CH_3 asymmetric stretching vibrations are expected to be at 2950–3050 cm^{-1} and the CH_3 symmetric vibrations to be at 2900–2950 cm^{-1} [48, 49]. For compound **2**, the symmetric stretching modes were seen at 2949 and 2934 cm^{-1} in the IR spectrum and at 2938 cm^{-1} in the Laser-Raman spectrum. They were calculated to be at 2943 (B3LYP)/2929 (M06-2X) and 2934 (B3LYP)/2916 (M06-2X) cm^{-1}, again showing that the B3LYP method gives better agreement with experimental values.

4.3.4. Quinazolinone Group Vibrations. In quinazoline compounds, C=N stretching bands are generally observed at 1627–1566 cm^{-1} [51–53], while for conjugated azines the νC=N mode has been reported to appear around 1553 cm^{-1} [54]. For compound **2**, the (C4=N13) bands were seen at 1605 (IR)/1609 (Raman) and 1570 (IR)/1578 (Raman) cm^{-1} and calculated to be at 1593 (B3LYP)/1623 (M06-2X) and 1580 (B3LYP)/1601 (M06-2X) cm^{-1}. Again, the B3LYP method provides the closer fit with the experimental values. Other C–N stretching bands [55] generally occur around 1100–1300 cm^{-1}, while aromatic C–H stretching typically exhibits several weak to moderate bands above 3000 cm^{-1} [56]. Aromatic C–H in-plane bending vibrations usually occur in the region of 1390–990 cm^{-1} and are very useful for characterization purposes [57], while C–H out-of-plane deformations generally occur around 1000 to 700 cm^{-1}, with bands having higher wavenumbers being weaker than those absorbing at lower wavenumbers [58]. Table 2 shows the experimental and calculated values for compound **2**.

Ring C=C stretching vibrations usually occur around 1625–1430 cm^{-1} [59]. For benzenoid compounds there are two or three bands due to skeletal vibrations; the strongest band is at *ca.* 1500 cm^{-1}. The observed and calculated values for compound **2** are shown in Table 2.

4.4. HOMO-LUMO Analysis. Chemical stability is mainly influenced by the frontier orbitals (HOMO and LUMO). The HOMO represents electron-donating capability, while the LUMO represents electron accepting capability [60]. The HOMO and LUMO energies of **2** were calculated by the B3LYP/6-311++G(d,p) (Figure 5; positive phase represented in red and negative phase represented in green) and M06-2X/6-311++G(d,p) methods. A large HOMO-LUMO gap implies a chemically "hard" molecule and a small HOMO-LUMO gap implies a "soft" molecule. The chemical reactivity of a molecule is also related to its "hardness," molecules with lower HOMO-LUMO gaps being more reactive [61]. The frontier molecular orbital energy gap therefore helps in understanding the kinetic stability and reactivity of molecules [62, 63].

The HOMO-LUMO energy gap calculated for compound **2** is 5.119590424 e.V by B3LYP/6-311++G(d,p) and 7.459788024 e.V by M06-2X/6-311++G(d,p). This energy gap reflects the chemical activity of the molecule and influences its biological activity. As is evident from Figure 5, the HOMO is located on the quinazoline rings, the acetylamino group, and over the C1=O14 carbonyl group. The LUMO is more focused on the quinazoline ring and the C1=O14 carbonyl group and partially over the C29 atom.

The ionization energy (I) and electron affinity (A) can be expressed by HOMO and LUMO orbital energies as $I = -E_{\mathrm{HOMO}}$ and $A = -E_{\mathrm{LUMO}}$. The global hardness $\eta = 1/2(E_{\mathrm{LUMO}} - E_{\mathrm{HOMO}})$. The ionization energy, along with electron affinity, can be used to give electronic chemical potential, $\mu = 1/2(E_{\mathrm{LUMO}} + E_{\mathrm{HOMO}})$, the global electrophilicity index $\psi = \mu^2/2\eta$, and the softness $\zeta = 1/\eta$ [64]. Such parameters were calculated and are tabulated in Table 3. The ionization

Table 3: Comparison of HOMO-LUMO energy gaps and related molecular properties of **2**.

Molecular properties	B3LYP/6-311++G(d,p)	M06-2X/6-311++G(d,p)
Energies (a.u)	−932.460118	−932.085968
E_{HOMO} (e.V)	−6.938958	−8.084022128
E_{LUMO} (e.V)	−1.819367576	−0.828865336
Energy gap (e.V)	5.119590424	7.459788024
Ionization potential (I)	6.938958	8.084022128
Electron affinity (A)	1.819367576	0.828865336
Global hardness (η)	2.5597995212	3.627677972
Chemical potential (μ)	4.37912788	4.4564433732
Electrophilicity (ψ)	3.74581419	2.73727385
Softness (ζ)	0.390655593	0.2756584261
Dipole moment (debye)	2.9159	2.8371

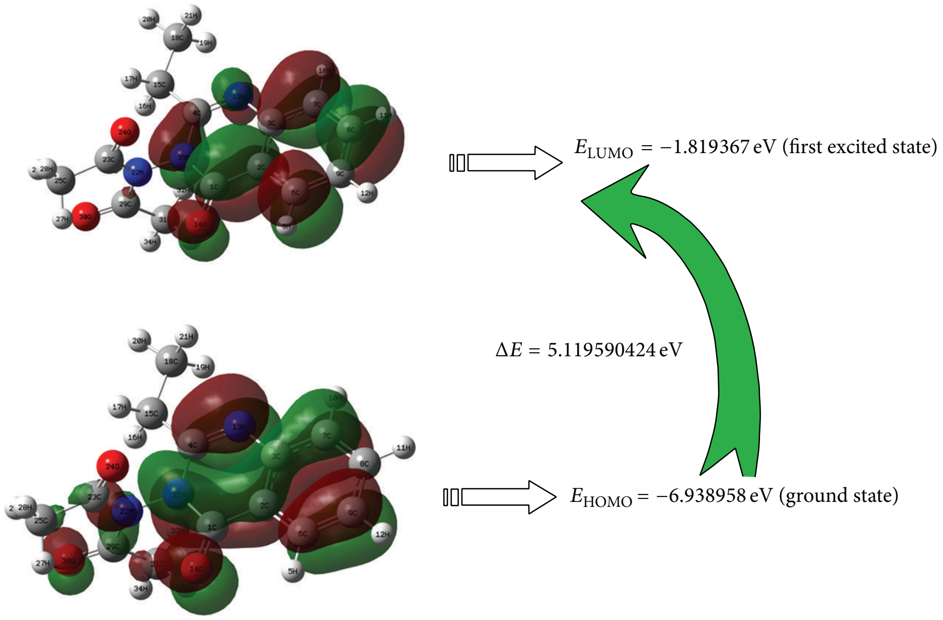

Figure 5: Calculated HOMO-LUMO plots of title compound **2**.

potentials given by the B3LYP and M06-2X methods for **2** are 6.938958 eV and 8.084022128 eV, respectively. The HOMO and LUMO energies of 2-quinazolinone and 4-quinazolinone calculated by B3LYP/6-311G(d), 6-311+G(d,p), and 6-311++G(d,p) sets have been reported previously [58]. For both molecules, LUMOs are distributed uniformly over the entire molecules and show antibonding character. For both molecules, the HOMOs are shifted mainly towards the pyrimidinone and some part of the benzene ring [58].

5. Conclusion

In this work, the vibrational modes of newly synthesized 3-(diacetylamino)-2-ethyl-3*H*-quinazolin-4-one (**2**) were studied experimentally by use of FT-IR and Laser-Raman spectra and computationally using DFT/B3LYP and M06-2X methods. The vibrational harmonic frequencies, optimized geometric parameters, molecular orbital energies, and other properties related to HOMO and LUMO energy values of compound **2** were calculated using DFT/B3LYP and M06-2X methods with the 6-311++G(d,p) basis set. The assignments of the vibrational frequencies were made with the help of potential energy distribution (PED) analysis using VEDA 4 software. The theoretical optimized geometric parameters and vibrational frequencies have been found to be in good agreement with the corresponding experimental data and results in the literature. The calculated HOMO and LUMO orbitals and their energies have been used to gain understanding of charge transfer within compound **2**.

Conflict of Interests

The authors declare that there is no conflict of interests regarding the publication of this paper.

Acknowledgment

The authors would like to extend their appreciation to the Deanship of Scientific Research at King Saud University for funding this research through the research group project RGP-VPP-239.

References

[1] V. Alagarsamy, V. R. Solomon, and K. Dhanabal, “Synthesis and pharmacological evaluation of some 3-phenyl-2-substituted-3H-quinazolin-4-one as analgesic, anti-inflammatory agents,” *Bioorganic and Medicinal Chemistry*, vol. 15, no. 1, pp. 235–241, 2007.

[2] R. Rohini, P. M. Reddy, K. Shanker, A. Hu, and V. Ravinder, “Antimicrobial study of newly synthesized 6-substituted indolo[1,2-*c*]quinazolines,” *European Journal of Medicinal Chemistry*, vol. 45, no. 3, pp. 1200–1205, 2010.

[3] V. Gupta, S. K. Kashaw, V. Jatav, and P. Mishra, “Synthesis and antimicrobial activity of some new 3-[5-(4-substituted) phenyl-1,3,4-oxadiazole-2yl]-2- styrylquinazoline-4(3*H*)-ones,” *Medicinal Chemistry Research*, vol. 17, no. 2, pp. 205–211, 2008.

[4] V. Chandregowda, A. K. Kush, and G. C. Reddy, “Synthesis and *in vitro* antitumor activities of novel 4-anilinoquinazoline derivatives,” *European Journal of Medicinal Chemistry*, vol. 44, no. 7, pp. 3046–3055, 2009.

[5] M. F. Abdel-Megeed, B. E. Badr, M. M. Azaam, and G. A. El-Hiti, “Synthesis, antimicrobial and anticancer activities of a novel series of diphenyl 1-(pyridin-3-yl)ethylphosphonates,” *Bioorganic and Medicinal Chemistry*, vol. 20, no. 7, pp. 2252–2258, 2012.

[6] S. Sasmal, G. Balaji, H. R. K. Reddy et al., “Design and optimization of quinazoline derivatives as melanin concentrating hormone receptor 1 (MCHR1) antagonists,” *Bioorganic & Medicinal Chemistry Letters*, vol. 22, no. 9, pp. 3157–3162, 2012.

[7] M. S. Malamas and J. Millen, “Quinazolineacetic acids and related analogues as aldose reductase inhibitors,” *Journal of Medicinal Chemistry*, vol. 34, no. 4, pp. 1492–1503, 1991.

[8] J. Ma, B. Han, J. Song et al., “Efficient synthesis of quinazoline-2,4(1*H*,3*H*)-diones from CO_2 and 2-aminobenzonitriles in water without any catalyst,” *Green Chemistry*, vol. 15, no. 6, pp. 1485–1489, 2013.

[9] L. Xu, Y. Jiang, and D. Ma, “Synthesis of 3-substituted and 2,3-disubstituted quinazolinones via Cu-catalyzed aryl amidation,” *Organic Letters*, vol. 14, no. 4, pp. 1150–1153, 2012.

[10] M. Adib, E. Sheikhi, and H. R. Bijanzadeh, “One-pot three-component synthesis of 4(3*H*)-quinazolinones from benzyl halides, isatoic anhydride, and primary amines,” *Synlett*, vol. 23, no. 1, Article ID D13011ST, pp. 85–88, 2012.

[11] K. Smith, G. A. El-Hiti, and M. F. Abdel-Megeed, “Regioselective lithiation of chiral 3-acylamino-2-alkylquinazolin-4(3*H*)-ones: application in synthesis,” *Synthesis*, no. 13, pp. 2121–2130, 2004.

[12] G. A. El-Hiti, “A simple procedure for the side-chain substitution of 2-alkyl-3*H*-quinazoline-4-thiones: application in synthesis,” *Synthesis*, no. 3, pp. 363–368, 2004.

[13] G. A. El-Hiti, “Application of organolithium in organic synthesis: a simple and convenient procedure for the synthesis of more complex 6-substituted 3*H*-quinazolin-4-ones,” *Monatshefte fur Chemie*, vol. 135, no. 3, pp. 323–331, 2004.

[14] G. A. El-Hiti, A. S. Hegazy, M. H. Alotaibi, and M. D. Ajarim, “Reactions of organolithium reagents with quinazoline derivatives,” *Arkivoc*, vol. 2012, no. 7, pp. 35–78, 2012.

[15] K. Smith, G. A. El-Hiti, and S. A. Hegazy, “A simple and convenient procedure for lithiation and side-chain substitution of 2-alkyl-4-(methylthio)quinazolines and 2-alkyl-4-methoxyquinazolines,” *Synthesis*, no. 17, pp. 2951–2961, 2005.

[16] G. M. Sheldrick, “Phase annealing in SHELX-90: direct methods for larger structures,” *Acta Crystallographica Section A: Foundations of Crystallography*, vol. 46, no. 6, pp. 467–473, 1990.

[17] G. M. Sheldrick, *SHELXS-97, Program for Crystal Structure Refinement*, Universität Göttingen, Göttingen, Germany, 1997.

[18] M. A. Palafox, V. K. Rastogi, R. P. Tanwar, and L. Mittal, “Vibrational frequencies and structure of 2-thiouracil by Hartree-Fock, post-Hartree-Fock and density functional methods,” *Spectrochimica Acta Part A: Molecular and Biomolecular Spectroscopy*, vol. 59, no. 11, pp. 2473–2486, 2003.

[19] G. N. Ten, V. V. Nechaev, A. N. Pankratov, V. I. Berezin, and V. I. Baranov, “Effect of hydrogen bonding on the structure and vibrational spectra of the complementary pairs of nucleic acid bases. II. adenine-thymine,” *Journal of Structural Chemistry*, vol. 51, no. 5, pp. 854–861, 2010.

[20] Ç. Çırak and N. Koç, “Molecular structure and effects of intermolecular hydrogen bonding on the vibrational spectrum of trifluorothymine, an antitumor and antiviral agent,” *Journal of Molecular Modeling*, vol. 18, no. 9, pp. 4453–4464, 2012.

[21] M. A. Palafox, G. Tardajos, A. Guerrero-Martínez et al., “FT-IR, FT-Raman spectra, density functional computations of the vibrational spectra and molecular geometry of biomolecule 5-aminouracil,” *Chemical Physics*, vol. 340, no. 1–3, pp. 17–31, 2007.

[22] J. S. Singh, “FTIR and Raman spectra and fundamental frequencies of biomolecule: 5-methyluracil (thymine),” *Journal of Molecular Structure*, vol. 876, no. 1–3, pp. 127–133, 2008.

[23] M. H. Jamróz, J. C. Dobrowolski, and R. Brzozowski, “Vibrational modes of 2,6-, 2,7-, and 2,3-diisopropylnaphthalene. A DFT study,” *Journal of Molecular Structure*, vol. 787, no. 1–3, pp. 172–183, 2006.

[24] Ç. Çırak, Y. Sert, and F. Ucun, “Experimental and computational study on molecular structure and vibrational analysis of a modified biomolecule: 5-Bromo-2′-deoxyuridine,” *Spectrochimica Acta Part A: Molecular and Biomolecular Spectroscopy*, vol. 92, no. 6, pp. 406–414, 2012.

[25] Y. Zhao and D. G. Truhlar, “The M06 suite of density functionals for main group thermochemistry, thermochemical kinetics, noncovalent interactions, excited states, and transition elements: two new functionals and systematic testing of four M06-class functionals and 12 other functionals,” *Theoretical Chemistry Accounts*, vol. 120, no. 1–3, pp. 215–241, 2008.

[26] K. Helios, R. Wysokiński, A. Pietraszko, and D. Michalska, “Vibrational spectra and reinvestigation of the crystal structure of a polymeric copper(II)-orotate complex, $[\mathrm{Cu}(\mu\text{-HOr})(\mathrm{H_2O})2]n$: the performance of new DFT methods, M06 and M05-2X, in theoretical studies,” *Vibrational Spectroscopy*, vol. 55, no. 2, pp. 207–215, 2011.

[27] J. Gu, J. Wang, and J. Leszczynski, “Stacking and H-bonding patterns of dGpdC and dGpdCpdG: performance of the M05-2X and M06-2X Minnesota density functionals for the single strand DNA,” *Chemical Physics Letters*, vol. 512, no. 1–3, pp. 108–112, 2011.

[28] K. H. Lemke and T. M. Seward, “Thermodynamic properties of carbon dioxide clusters by M06-2X and dispersion-corrected

B2PLYP-D theory," *Chemical Physics Letters*, vol. 573, no. 6, pp. 19–23, 2013.

[29] E. I. Paulraj and S. Muthu, "Spectroscopic studies (FTIR, FT-Raman and UV), potential energy surface scan, normal coordinate analysis and NBO analysis of (2*R*,3*R*,4*R*,5*S*)-1-(2-hydroxyethyl)-2-(hydroxymethyl) piperidine-3,4,5-triol by DFT methods," *Spectrochimica Acta Part A: Molecular and Biomolecular Spectroscopy*, vol. 108, no. 5, pp. 38–49, 2013.

[30] U. Yadava, M. Singh, and M. Roychoudhury, "Gas-phase conformational and intramolecular π-π interaction studies on some pyrazolo[3,4-*d*]pyrimidine derivatives," *Computational and Theoretical Chemistry*, vol. 977, no. 1–3, pp. 134–139, 2011.

[31] C. N. Ramachandran and E. Ruckenstein, "Density functional theoretical studies of the isomers of croconic acid and their dimers," *Computational and Theoretical Chemistry*, vol. 973, no. 1–3, pp. 28–32, 2011.

[32] Y. Sert, Ç. Çırak, and F. Ucun, "Vibrational analysis of 4-chloro-3-nitrobenzonitrile by quantum chemical calculations," *Spectrochimica Acta Part A: Molecular and Biomolecular Spectroscopy*, vol. 107, no. 4, pp. 248–255, 2013.

[33] A. Frish, A. B. Nielsen, and A. J. Holder, *Gauss View User Manual*, Gaussian Inc, Pittsburg, Pa, USA, 2001.

[34] W. H. James, E. G. Buchanan, C. W. Müller et al., "Evolution of amide stacking in larger γ-peptides: triamide H-bonded cycles," *Journal of Physical Chemistry A*, vol. 115, no. 47, pp. 13783–13798, 2011.

[35] M. J. Frisch, G. W. Trucks, H. B. Schlegel et al., *Gaussian 03, Revision D.01*, Gaussian, Wallingford, Conn, USA, 2004.

[36] M. H. Jamróz, *Vibrational Energy Distribution Analysis VEDA 4*, 2004.

[37] M. H. Jamróz, "Vibrational energy distribution analysis (VEDA): scopes and limitations," *Spectrochimica Acta Part A: Molecular and Biomolecular Spectroscopy*, vol. 114, no. 10, pp. 220–230, 2013.

[38] H. Arslan and Ö. Algül, "Vibrational spectrum and assignments of 2-(4-methoxyphenyl)-1*H*-benzo[*d*]imidazole by ab initio Hartree-Fock and density functional methods," *Spectrochimica Acta Part A: Molecular and Biomolecular Spectroscopy*, vol. 70, no. 1, pp. 109–116, 2008.

[39] C. Irak, S. Demir, F. Ucun, and O. Ubuk, "Experimental and theoretical study on the structure and vibrational spectra of β-2-aminopyridinium dihydrogenphosphate," *Spectrochimica Acta Part A: Molecular and Biomolecular Spectroscopy*, vol. 79, no. 3, pp. 529–532, 2011.

[40] G. A. El-Hiti, K. Smith, A. S. Hegazy, M. D. Ajarim, and B. M. Kariuki, "Crystal structure of 2-[4-(methylsulfanyl)quinazolin-2-yl]-1-phenylethanol," *Acta Crystallographica Section E: Crystallographic Communications*, vol. 70, no. 11, p. o1101, 2014.

[41] C. Y. Panicker, H. T. Varghese, K. R. Ambujakshan et al., "Vibrational spectra and computational study of 3-amino-2-phenyl quinazolin-4(3*H*)-one," *Journal of Molecular Structure*, vol. 963, no. 2-3, pp. 137–144, 2010.

[42] C. Y. Panicker, H. T. Varghese, K. R. Ambujakshan et al., "Ab initio and density functional theory studies on vibrational spectra of 3-{[(4-methoxyphenyl)methylene]amino}-2-phenylquinazolin-4(3H)-one," *European Journal of Chemistry*, vol. 1, no. 1, pp. 37–43, 2010.

[43] J. P. Jasinski, J. A. Golen, A. S. Praveen, H. S. Yathirajan, and B. Narayana, "Methyl 3,5-dibromo-2-diacetylaminobenzoate," *Acta Crystallographica Section E: Crystallographic Communications*, vol. 67, no. 9, p. o2503, 2011.

[44] C.-L. He, Z.-M. Du, Z.-Q. Tang, X.-M. Cong, and L.-Q. Meng, "*N*-(1-Diacetylamino-1*H*-tetrazol-5-yl)acetamide," *Acta Crystallographica, Section E: Crystallographic Communications*, vol. 65, part 8, article o1902, 2009.

[45] G. Socrates, *Infrared and Raman Characteristic Group Frequencies: Tables and Charts*, John Wiley & Sons, Chichester, UK, 3rd edition, 2004.

[46] C. Y. Panicker, H. T. Varghese, K. R. Ambujakshan et al., "FT-IR and FT-Raman spectra and *ab initio* calculations of 3-{[(2-hydroxyphenyl) methylene]amino}-2-phenylquinazolin-4(3*H*)-one," *Journal of Raman Spectroscopy*, vol. 40, no. 9, pp. 1262–1273, 2009.

[47] C. Y. Panicker, H. T. Varghese, K. R. Ambujakshan et al., "FT-IR, FT-Raman and DFT calculations of 3-[(4-fluorophenyl)methylene] amino-2-phenylquinazolin-4(3*H*)-one," *Journal of Raman Spectroscopy*, vol. 40, no. 5, pp. 527–536, 2009.

[48] N. P. G. Roeges, *A Guide to the Complete Interpretation of Infrared Spectra of Organic Structures*, John Wiley & Sons, New York, NY, USA, 1994.

[49] P. Larkin, *Infrared and Raman Spectroscopy; Principles and Spectral Interpretation*, Elsevier, Waltham, Mass, USA, 1st edition, 2011.

[50] C. Y. Panicker, H. T. Varghese, M. Nair, K. Raju, M. Laila, and G. M. Warrier, "Vibrational spectroscopic studies and ab initio calculations of 3-nitroacetanilide," *Oriental Journal of Chemistry*, vol. 25, no. 3, pp. 643–647, 2009.

[51] I. Yalçin, E. Şener, T. Özden, S. Özden, and A. Akin, "Synthesis and microbiological activity of 5-methyl-2-[*p*-substituted phenyl]benzoxazoles," *European Journal of Medicinal Chemistry*, vol. 25, no. 8, pp. 705–708, 1990.

[52] R. Saxena, L. D. Kandpal, and G. N. Mathur, "Synthesis and characterization of poly(benzobisthiazole)s derived from halogenated phthalic acid and isophthalic acid," *Journal of Polymer Science, Part A: Polymer Chemistry*, vol. 40, no. 22, pp. 3959–3966, 2002.

[53] R. M. Silverstein and F. X. Webster, *Spectrometric Identification of Organic Compound*, John Wiley & Sons, Singapore, 6th edition, 2003.

[54] J. M. Engasser and C. Horvath, "Electrostatic effects on the kinetics of bound enzymes," *Biochemical Journal*, vol. 145, no. 3, pp. 431–435, 1975.

[55] S. Kundoo, A. N. Banerjee, P. Saha, and K. K. Chattopadhyay, "Synthesis of crystalline carbon nitride thin films by electrolysis of methanol-urea solution," *Materials Letters*, vol. 57, no. 15, pp. 2193–2197, 2003.

[56] J. Coates and R. A. Meyers, *Introduction to Infrared Spectrum. A Practical Approach*, John Wiley & Sons, Chichester, UK, 2000.

[57] M. Pagannone, B. Fornari, and G. Mattei, "Molecular structure and orientation of chemisorbed aromatic carboxylic acids: surface enhanced Raman spectrum of benzoic acid adsorbed on silver sol," *Spectrochimica Acta Part A: Molecular Spectroscopy*, vol. 43, no. 5, pp. 621–625, 1987.

[58] S. R. Kumar, N. Vijay, K. Amarendra, P. Onkar, and S. Leena, "Theoretical studies on the isomers of quinazolinone by first principles," *Research Journal of Recent Sciences*, vol. 1, no. 3, pp. 11–18, 2012.

[59] D. L. Pavia, G. M. Lampman, and G. S. Kriz, *Introduction to Spectroscopy*, Harcourt College Publishers, 2001.

[60] E. Kavitha, N. Sundaraganesan, S. Sebastian, and M. Kurt, "Molecular structure, anharmonic vibrational frequencies and NBO analysis of naphthalene acetic acid by density functional

theory calculations," *Spectrochimica Acta Part A: Molecular and Biomolecular Spectroscopy*, vol. 77, no. 3, pp. 612–619, 2010.

[61] K. Chaitanya, "Molecular structure, vibrational spectroscopic (FT-IR, FT-Raman), UV-vis spectra, first order hyperpolarizability, NBO analysis, HOMO and LUMO analysis, thermodynamic properties of benzophenone 2,4-dicarboxylic acid by ab initio HF and density functional method," *Spectrochimica Acta—Part A: Molecular and Biomolecular Spectroscopy*, vol. 86, pp. 159–173, 2012.

[62] E. Kavitha, N. Sundaraganesan, and S. Sebastian, "Molecular structure, vibrational spectroscopic and HOMO, LUMO studies of 4-nitroaniline by density functional method," *Indian Journal of Pure & Applied Physics*, vol. 48, no. 1, pp. 20–30, 2010.

[63] A. Jayaprakash, V. Arjunan, and S. Mohan, "Vibrational spectroscopic, electronic and quantum chemical investigations on 2,3-hexadiene," *Spectrochimica Acta Part A: Molecular and Biomolecular Spectroscopy*, vol. 81, no. 1, pp. 620–630, 2011.

[64] M. Govindarajan, M. Karabacak, A. Suvitha, and S. Periandy, "FT-IR, FT-Raman, ab initio, HF and DFT studies, NBO, HOMO-LUMO and electronic structure calculations on 4-chloro-3-nitrotoluene," *Spectrochimica Acta—Part A: Molecular and Biomolecular Spectroscopy*, vol. 89, pp. 137–148, 2012.

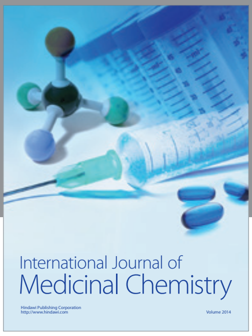
International Journal of
Medicinal Chemistry

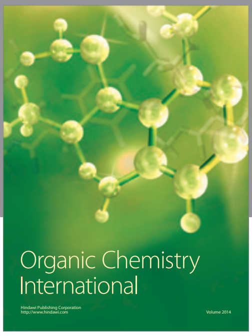
Organic Chemistry
International

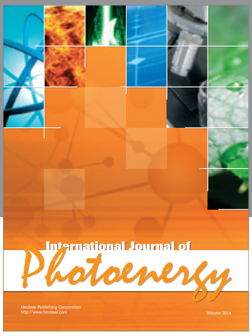
International Journal of
Photoenergy

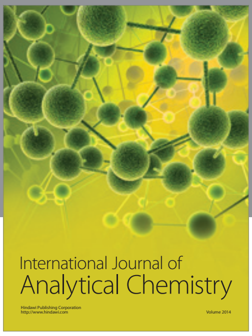
International Journal of
Analytical Chemistry

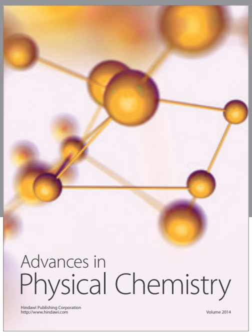
Advances in
Physical Chemistry

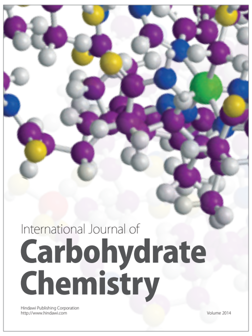
International Journal of
Carbohydrate Chemistry

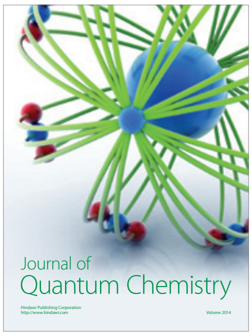
Journal of
Quantum Chemistry


The Scientific World Journal

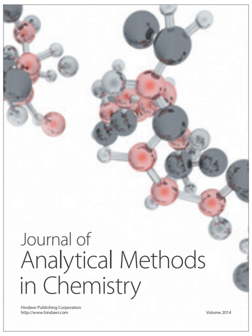
Journal of
Analytical Methods in Chemistry


Journal of
Spectroscopy

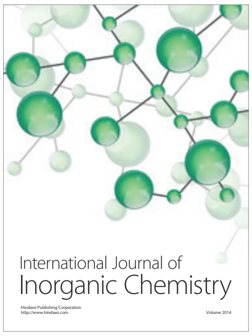
International Journal of
Inorganic Chemistry


International Journal of
Electrochemistry

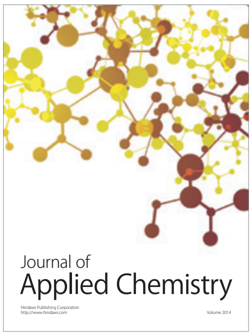
Journal of
Applied Chemistry

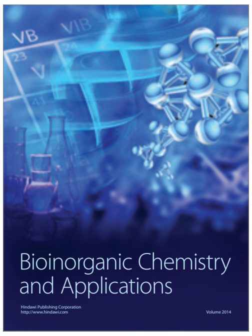
Bioinorganic Chemistry
and Applications


Journal of
Theoretical Chemistry

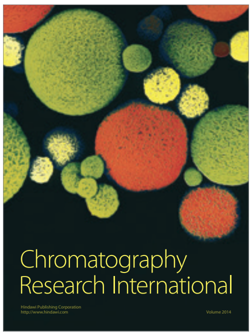
Chromatography
Research International


Journal of
Catalysts


Journal of
Chemistry


International Journal of
Spectroscopy